19th Brazilian Congress of Thermal Sciences and Engineering
November 6th–10th, 2022, Bento Gonçalves - RS - Brazil

ENC-2022-XXXX
COMPUTATIONAL ANALYSIS OF THE FLOW IN A BACKWARD-FACING STEP WITH AN EXPANSION RATIO OF 1.94

Deidson Vilhena Santos
Álvaro Luiz de Bortoli
Federal University of Rio Grande do Sul - UFRGS. Av. Bento Gonçalves, 9500 - Agronomia, Porto Alegre - RS, 90.650-001
deidsonjc@hotmail.com; dbortoli@mat.ufrgs.br

Abstract. *Flows over a backward-facing step (BFS) make up a branch of fluid mechanics in which many characteristics of flows are investigated. In this work, a Computational Fluid Dynamics (CFD) analysis of the flow over a BFS with expansion ratio of 1.94 is presented. The flow equations are the set of incompressible Navier-Stokes equations, whose pressure is given by the Poisson equation. The numerical solution is obtained by the simplified Runge-Kutta method with three steps, and the equations are discretized by the centered finite difference scheme. A grid independence analysis is done for four different grid sizes, and it is observed that the optimal grid condition is for 300x25 points. Numerical results are given for five Reynolds numbers (50, 100, 200, 500, and 800), which are compared with literature data through longitudinal velocity profiles in two different sections of the duct. The results of this work showed good agreement with the literature data.*

Keywords: *Computational Fluid Dynamics, Runge-Kutta Method, Backward-Facing Step, Navier-Stokes Equations.*

1. INTRODUCTION

Flows over a Backward-Facing Step (BFS) have been widely studied recently for their applications in engineering problems, characterizing a geometric domain similar to that of these problems have (Montazer *et al.*, 2018). Therefore, despite their simple geometry, flows in BFS serve as prototypes to investigate flow characteristics such as flow stabilization, shear layer, recirculation zone, boundary layer separation, and mixing pattern (Liakos and Malamataris, 2015).

For example, literature results have shown that the heat transfer effects are most effective in the recirculation zone (Chen *et al.*, 2018), so a significant change in this region can alter the effectiveness of this process. Also, in the combustion process resulting from the injection of nanoparticles into a base fuel, an efficient mixing of the reagents is necessary (Nong *et al.*, 2020). Thus, the characteristics of the flow mixing pattern are of paramount importance for combustion efficiency. Furthermore, in the transport of heavy oils through pipelines (Zambrano *et al.*, 2017), a well-developed flow is required in the shear layer to maintain a good velocity intensity in this region.

For this reason, this work develops a mathematical-computational model to investigate the flow properties in a BFS whose expansion ratio (ER) is given by $ER = 1.94$. As the Reynolds number directly influences the disturbances in the flow, simulations are performed for five values of this number: 50, 100, 200, 500, and 800.

2. MATHEMATICAL MODELING

2.1 Backward-Facing Step Geometry

Figure 1 shows the geometric domain which is subject of study in this work.

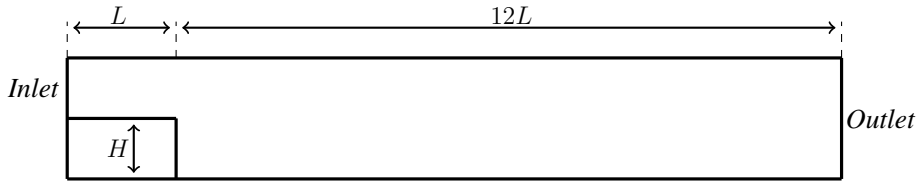

Figure 1. BFS geometry of this work.

Such geometry is called *backward-facing step* (BFS), where the parameters shown in the figure, with their proportions, were taken according to the work of (Silva and Coutinho, 2015).

The key parameter of this geometry is the value L, from which all other dimensions are taken. It represents the length of the step and the height of the duct. The height of the step is given by $H = 0.516$ and the distance from the step to the end of the duct is given by $12L$. In the present study, $L = 1.0$ is established, so the relation $ER = \frac{L}{H}$, called the *expansion ratio*, results in $ER = 1.94$.

2.2 Flow Equations

The model, dimensionless for incompressible fluids, consists of the Navier-Stokes equations to obtain the numerical simulation of the flow, which is composed of the continuity and momentum equations:

$$\vec{\nabla} \cdot \vec{u} = 0 \ , \tag{1}$$

$$\frac{\partial \vec{u}}{\partial t} + \vec{u}\vec{\nabla}\vec{u} = -\vec{\nabla}p + \frac{1}{Re}\vec{\nabla}^2\vec{u} \ , \tag{2}$$

where Re is the Reynolds number, a dimensionless number given by $Re = \dfrac{\rho V L}{\mu}$.

The pressure equation was obtained according to the work of Beleza (2003), achieving a form of the Poisson equation, which is given by:

$$\vec{\nabla}^2 p = -\left[\left(\frac{\partial u}{\partial x}\right)^2 + 2\frac{\partial u}{\partial y}\frac{\partial v}{\partial x} + \left(\frac{\partial v}{\partial y}\right)^2\right] - \frac{\partial D}{\partial t} + \frac{1}{Re}\vec{\nabla}^2 D \ , \tag{3}$$

where $D = \dfrac{\partial u}{\partial x} + \dfrac{\partial v}{\partial y}$.

Finally, the vorticity relation obtained from the model is given according to Pritchard (2011):

$$\omega = \frac{\partial v}{\partial x} - \frac{\partial u}{\partial y} \ . \tag{4}$$

2.3 Initial and Boundary Conditions

Constant velocity in the x direction and atmospheric pressure are provided for the initial condition, according to the work of Silva and Coutinho (2015), that is,

$$u(t_0) = 1.0 \ m/s \ ; \tag{5}$$

$$v(t_0) = 0.0 \ m/s \ ; \tag{6}$$

$$p(t_0) = p_0 = 10^5 \ Pa \ . \tag{7}$$

The boundary conditions are parabolic velocity at the entrance to the duct, according to Silva and Coutinho (2015). Non-slip conditions were imposed for the walls and Neumann conditions for the exit. For pressure, extrapolations were prescribed at all boundaries, except for the fluid outlet. Figure 2 summarizes all the boundary conditions of this work.

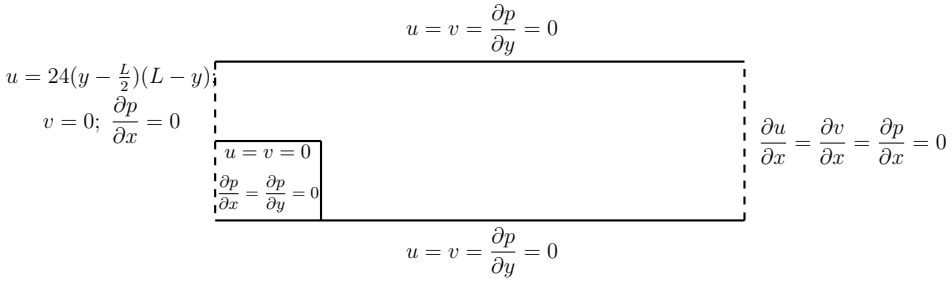

Figure 2. Boundary conditions for the BFS flow.

3. NUMERICAL SOLUTION PROCEDURE

The numerical procedure applied to the problem studied in this article is illustrated by the flowchart shown in Fig. 3.

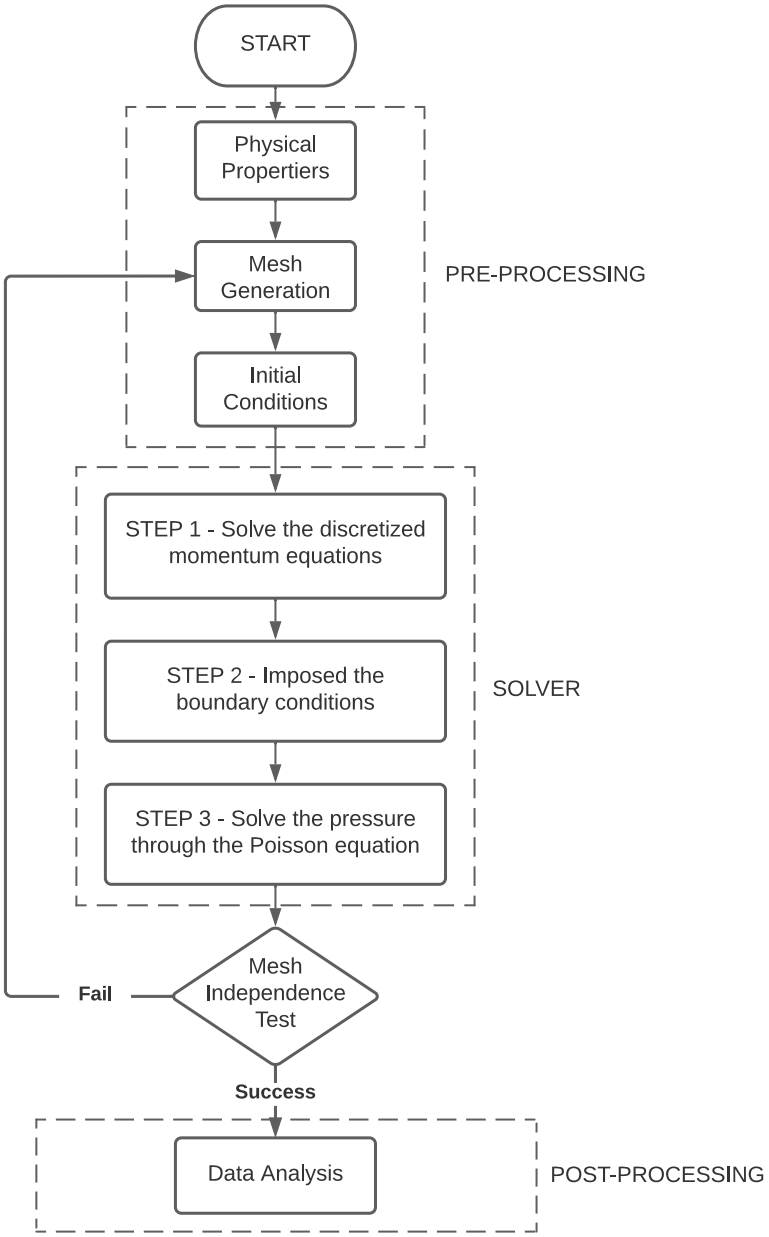

Figure 3. Flowchart of the numerical procedure of this work.

The computational mesh was of the structured type, containing 300×25 points, that is 7,500 nodes in total, as can be seen in Fig. 4. Refinement in the y-direction is given near the bottom of the domain. This is done because this is the region of greatest interest since the recirculation zone is located there.

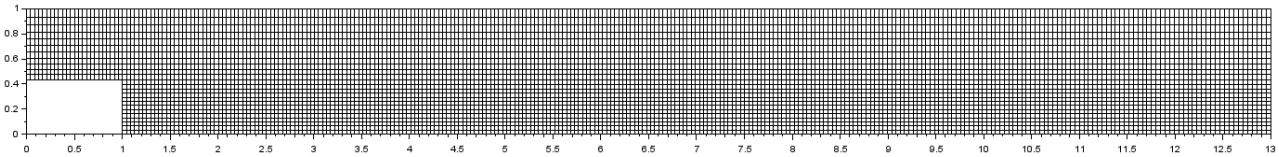

Figure 4. Computational mesh - 300×25 points.

The first and second order partial derivatives for the spatial variable were discretized by the centered Finite Difference

Method (Ferziger *et al.*, 2002). For example, for the partial derivatives in x, of an arbitrary variable f, we have:

$$\left(\frac{\partial f}{\partial x}\right)^{(n)}_{i,j,k} = \frac{f^{(n)}_{i+1,j,k} - f^{(n)}_{i-1,j,k}}{2\Delta x} + O(\Delta x^2)\ , \tag{8}$$

$$\left(\frac{\partial^2 f}{\partial x^2}\right)^{(n)}_{i,j,k} = \frac{f^{(n)}_{i+1,j,k} - 2f^{(n)}_{i,j,k} + f^{(n)}_{i-1,j,k}}{\Delta x^2} + O(\Delta x^2)\ , \tag{9}$$

where Δx, Δt and $O(\Delta x^2)$ represents, respectively, the spatial increment in x, the time step and the truncation error.

The numerical method used to obtain the solution of the system of equations was the Simplified Runge-Kutta Method (De Bortoli *et al.*, 2015). For a system $\frac{\partial \vec{W}}{\partial t} = \vec{R}$, this scheme is given by:

$$\overrightarrow{W}^{(0)}_{i,j,k} = \overrightarrow{W}^{(n)}_{i,j,k}\ ; \tag{10}$$

$$\overrightarrow{W}^{(r)}_{i,j,k} = \overrightarrow{W}^{(0)}_{i,j,k} - \alpha_r \Delta t \overrightarrow{R}^{(r-1)}_{i,j,k}\ , \quad r = 1, 2, 3; \tag{11}$$

$$\overrightarrow{W}^{(n+1)}_{i,j,k} = \overrightarrow{W}^{(3)}_{i,j,k}\ , \tag{12}$$

where Δt is the time step used in the numerical simulation, $\overrightarrow{W}$ represents the states of the system, and $\overrightarrow{R}$ represents the residue. The parameter r is the stage in the method, that are 3, and the coefficients α_r, called Runge-Kutta coefficients, are given by $\alpha_1 = 0.5$, $\alpha_2 = 0.5$, and $\alpha_3 = 1$. More than two steps are used to extend the stability region.

The states in time step n are stored in Runge-Kutta stage 0, according to Equation 10. The 3 stages are executed in Equation 11. Finally, the states in Runge-Kutta stage 3 are stored in time step $n + 1$.

4. RESULTS AND DISCUSSION

4.1 Grid Independence Study

Mesh refinement analysis based on longitudinal velocity was performed on two sections of the domain to investigate whether the numerical results are grid-independent. This analysis is presented in Fig. 5 and Fig. 6, for four grid sizes for $Re = 100$, where sections 1 and 2 are located at positions x = 1.5 and x = 2.0, respectively.

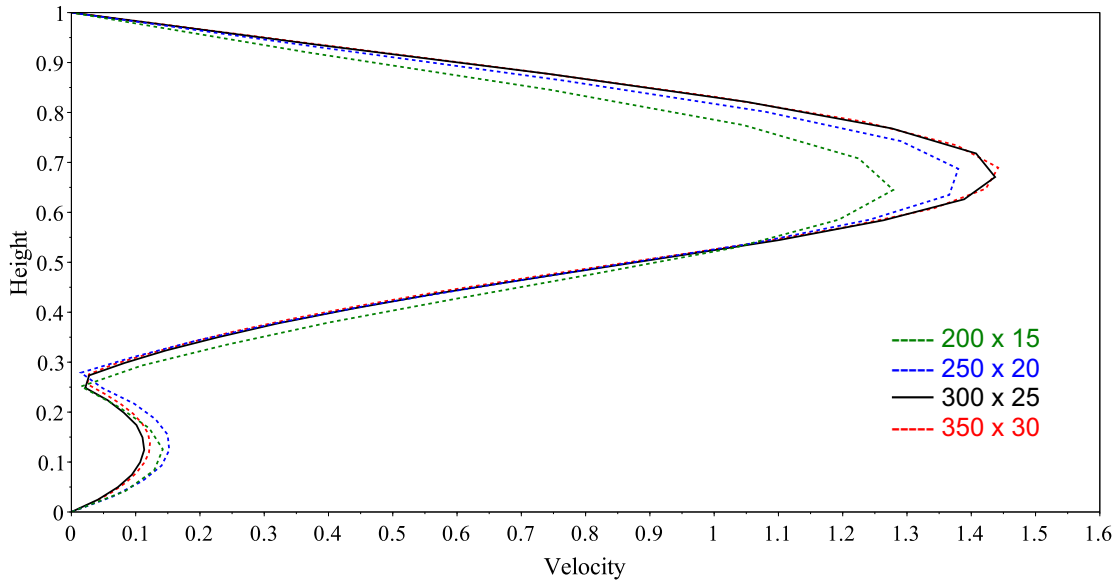

Figure 5. Mesh analysis in section 1 .

According to Fig. 5 and Fig. 6, the mesh with 300x25 points was selected due to the small variation of the results with a finer mesh.

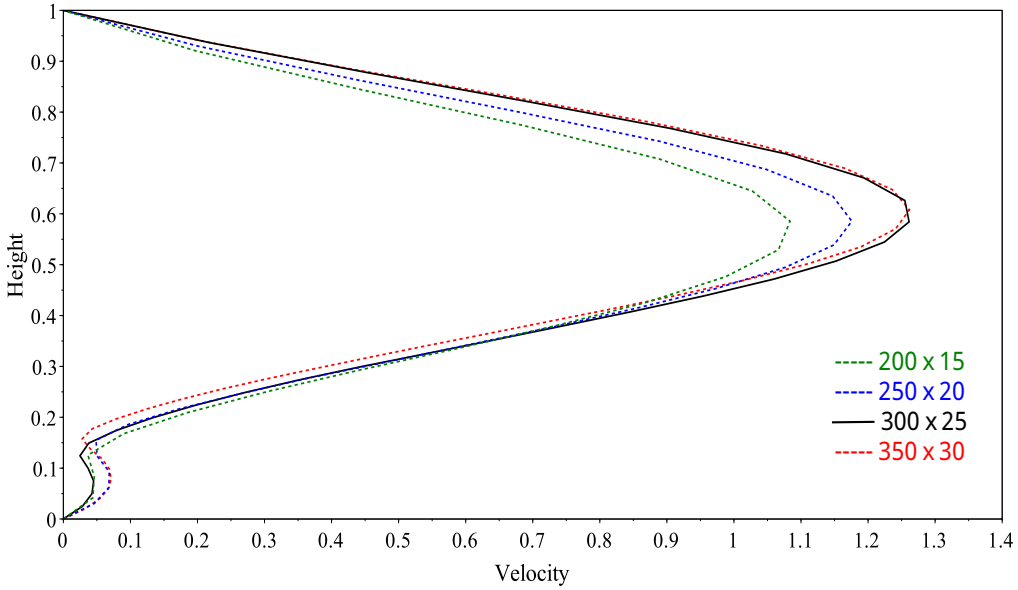

Figure 6. Grid analysis at the section 2.

4.2 Numerical Results

The results of the numerical simulation of this work are presented in Fig. 7, where the flow fields were taken to five different Reynolds numbers (50, 100, 200, 500, and 800).

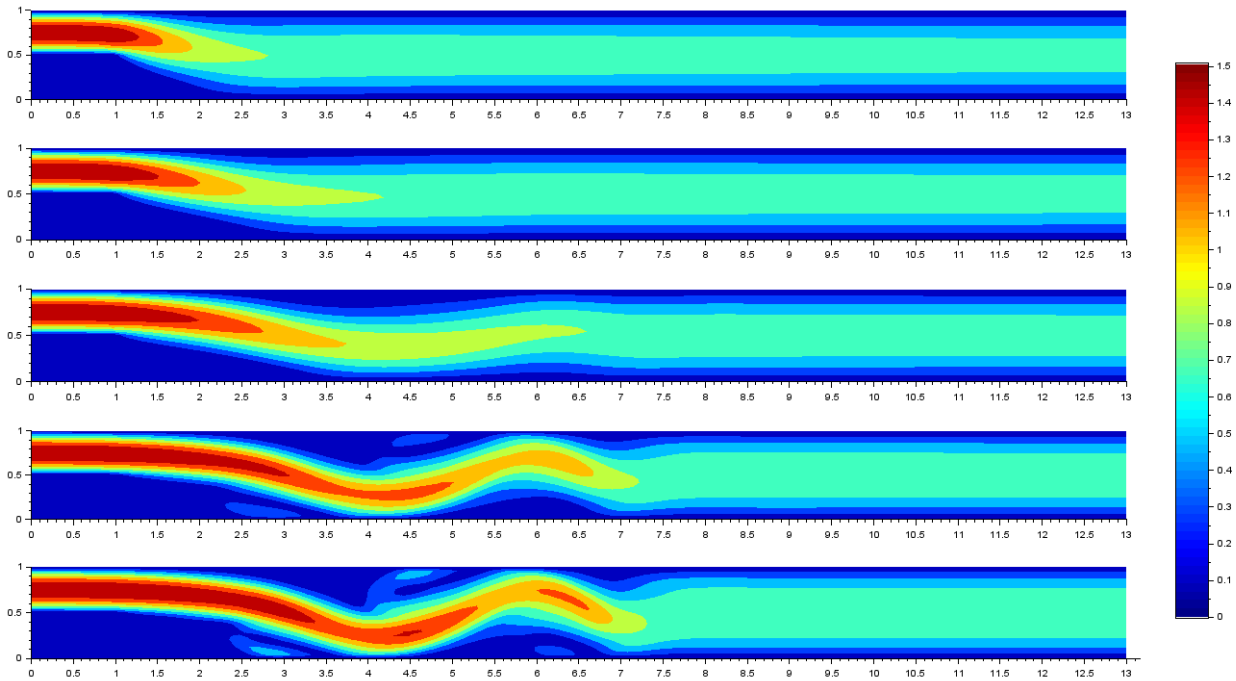

Figure 7. Flow fields for different Reynolds numbers.

Note that the increase in the Reynolds number generates disturbances in the flow. This fact happens because this dimensionless number relates the inertial to the viscous forces, directly influencing the contact of the fluid with the walls. Consequently, this increase in disturbances, causes the length of the recirculation zone to also increase, as can be seen in Fig. 7.

Therefore, next to the step, where is the recirculation zone, the velocity profiles were taken to compare the results of this work with the numerical data of Silva and Coutinho (2015). These profiles were calculated for $Re = 100$ because for values above 400 the influence of 3D geometry start to play a significant role. In Fig. 8, a comparison of the profiles is presented at position $x = 1.5$, obtaining good agreement with the literature data.

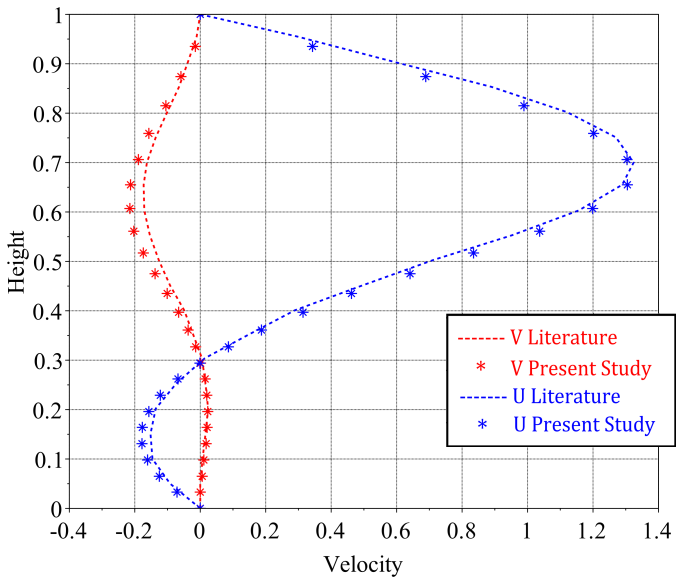

Figure 8. Comparison of velocity profiles with literature data for $Re = 100$ at position $x = 1.5$.

Figure 9 shows the comparison of velocity profiles at position $x = 2.0$. Although there are scattered values in some positions, generally good agreement was obtained.

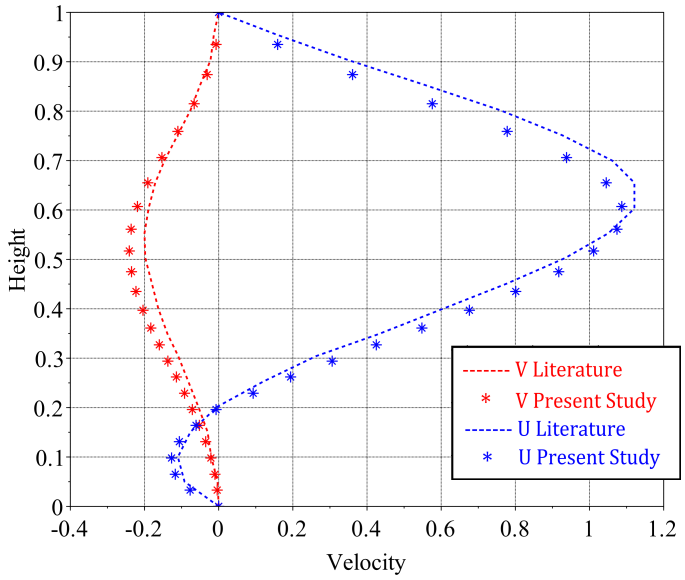

Figure 9. Comparison of velocity profiles with literature data for $Re = 100$ at position $x = 2.0$

5. CONCLUSIONS

The computational model developed in this work was validated by comparing the results with data from the literature and the mesh independence study, showing good agreement of the numerical simulation for flows over BFS.

There was good agreement between the results of this work and those of the literature, whose simulations were shown for five values of the Reynolds number: 50, 100, 200, 500, and 800. The comparison of the results was given for the velocity profiles at $Re = 100$. Such shows that the numerical model implemented in this work is compatible with those in the literature. The results lead to a good validation of the mathematical-computational model applied in this work.

Despite their simple geometry, backward-facing step flows serve as prototypes for flow optimization problems such as boundary layer separation, flow instabilities, and sudden expansions. As a future perspective, the procedure developed in

this work can be applied in the optimization, for example, of the mixture of combustion processes in combustors, of the transport speed in ducts, of the effects of lift and drag forces, of heat transfer in refrigeration and heat exchangers.

6. REFERENCES

Beleza, L.C., 2003. *Simulação de Movimento Sanguíneo na Artéria Carótida Usando Diferenças Finitas*. Dissertação de Mestrado, PPGMAP: Universidade Federal do Rio Grande do Sul.

Chen, L., Asai, K., Nonomura, T., Xi, G. and Liu, T., 2018. "A review of backward-facing step (bfs) flow mechanisms, heat transfer and control". *Thermal Science and Engineering Progress*, Vol. 6, pp. 194–216. doi: 10.1016/j.tsep.2018.04.004.

De Bortoli, A.L., Andreis, G. and Pereira, F., 2015. *Modeling and Simulation of Reactive Flows*. Elsevier Science Publishing Inc. ISBN 978-0-12-802974-9.

Ferziger, J.H., Perić, M. and Street, R.L., 2002. *Computational Methods for Fluid Dynamics*, Vol. 3. Springer-Verlag.

Liakos, A. and Malamataris, N.A., 2015. "Topological study of steady state, three dimensional flow over a backward facing step". *Computers & Fluids*, Vol. 118, pp. 1–18.

Montazer, E., Yarmand, H., Salami, E., Muhamad, M.R., Kazi, S.N. and Badarudin, A., 2018. "A brief review study of flow phenomena over a backward-facing step and its optimization". *Renewable and Sustainable Energy Reviews*, Vol. 82, pp. 994–1005. ISSN 1364-0321.

Nong, H., Hajizadeh, M.R. and Babazadeh, H., 2020. "Numerical modeling of paraffin melting expedition with considering nanoparticles through wavy duct". *Journal of Molecular Liquids*, Vol. 305, p. 112807. doi: 10.1016/j.molliq.2020.112807.

Pritchard, P.J., 2011. *Fox and McDonald's Introduction to Fluid Mechanics*. John Wiley & Sons. ISBN 9780470547557.

Silva, D.F. and Coutinho, A.L., 2015. "Practical implementation aspects of Galerkin reduced order models based on proper orthogonal decomposition for computational fluid dynamics". *Journal of the Brazilian Society of Mechanical Sciences and Engineering*, Vol. 37, No. 4, pp. 1309–1327.

Zambrano, H., Sigalotti, L.D.G., Klapp, J., Peña-Polo, F. and Bencomo, A., 2017. "Heavy oil slurry transportation through horizontal pipelines: experiments and CFD simulations". *International Journal of Multiphase Flow*, Vol. 91, pp. 130–141. ISSN 0301-9322.

7. RESPONSIBILITY NOTICE

The authors are solely responsible for the printed material included in this paper.